Mixed-Lineage Kinase 1 and Mixed-Lineage Kinase 3 Subtype-Selective Dihydronaphthyl[3,4-a]pyrrolo[3,4-c]carbazole-5-ones: Optimization, Mixed-Lineage Kinase 1 Crystallography, and Oral in Vivo Activity in 1-Methyl-4-phenyltetrahydropyridine Models

Robert L. Hudkins,*[,†] James L. Diebold,[†] Ming Tao,[†] Kurt A. Josef,[†] Chung Ho Park,[†] Thelma S. Angeles,[†] Lisa D. Aimone,[†] Jean Husten,[†] Mark A. Ator,[†] Sheryl L. Meyer,[†] Beverly P. Holskin,[†] John T. Durkin,[†] Alexander A. Fedorov,[‡] Elena V. Fedorov,[‡] Steven C. Almo,[‡] Joanne R. Mathiasen,[†] Donna Bozyczko-Coyne,[†] Michael S. Saporito,[†] Richard W. Scott,[†] and John P. Mallamo[†]

Discovery Research, Cephalon, Incorporated, 145 Brandywine Parkway, West Chester, Pennsylvania 19380, and Albert Einstein College of Medicine, Bronx, New York 10461

Received May 17, 2008

The optimization of the dihydronaphthyl[3,4-a]pyrrolo[3,4-c]carbazole-5-one R^2 and R^{12} positions led to the identification of the first MLK1 and MLK3 subtype-selective inhibitors within the MLK family. Compounds **14** (CEP-5104) and **16** (CEP-6331) displayed good potency for MLK1 and MLK3 inhibition with a greater than 30- to 100-fold selectivity for related family members MLK2 and DLK. Compounds **14** and **16** were orally active in vivo in a mouse MPTP biochemical efficacy model that was comparable to the first-generation pan-MLK inhibitor **1** (CEP-1347). The MLK1 structure−activity relationships were supported by the first-reported X-ray crystal structure of MLK1 bound with **16**.

Introduction

The mixed-lineage kinases (MLKs) are critical upstream activating components of the stress-activated c-jun-N-terminal kinase (JNK) pathway, and they function to phosphorylate MAP kinase kinases MKK4 and MKK7 of the cascade. MKK4 and MKK7 activate the JNKs (JNK1−3) that phosphorylate the transcription factor cJun on Ser^{63} and Ser^{73}, which is an early initiating event in the cell-death process.[2,3] c-Jun phosphorylation mediates neuronal apoptosis in response to a variety of stimuli, and it may contribute to the cell death that is associated with neurodegenerative pathological conditions.[2] In Parkinson's disease (PD), compelling postmortem evidence indicates that neuronal apoptosis may be the underlying mode of cell death of nigrostriatal dopaminergic neurons, which is a primary cause of the hallmark locomotor deficits in the disease (akinesia, tremor, and postural instability).[4] The characteristic features of PD suggest that a drug that is capable of attenuating nigrostriatal dopaminergic degeneration could theoretically slow the disease progression by providing therapy beyond that of neurotransmitter replacement, which is an elusive unmet medical need.

Our efforts in the design and synthesis of MLK inhibitors in the indolocarbazole class identified **1** (CEP-1347)[5] as a first-generation molecule that advanced through phase III clinical trials (Figure 1). **1** promoted neuronal survival in numerous in vitro and in vivo models[5a,6] including attenuating the loss of tyrosine hydroxylase (TH) immunoreactivity and dopamine (DA) transporter density in mice and monkeys following the administration of 1-methyl-4-phenyl-tetrahydropyridine (MPTP).[5a,7] The chemistry objective for a subsequent follow-on, second-generation compound was to identify a fully synthetic entity to circumvent requirements for the fermented glycosolyated natural product (+)K-252a (**2**), which has a lower molecular weight and enhanced pharmacokinetic properties. Recently, we reported our work that identified the MLK pharmacophore in (+)K-252a

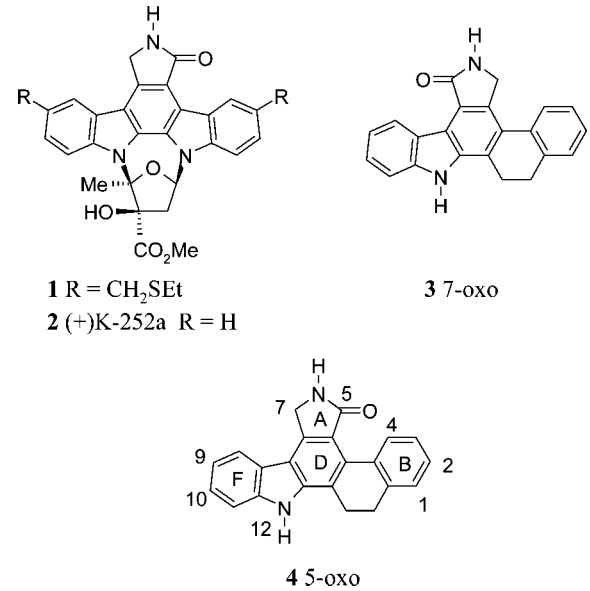

Figure 1. Structures of indolocarbazoles and dihydronaphthylcarbazoles.

that led to an MLK1 and MLK3 subtype-selective dihydronaphthyl[3,4-a]pyrrolo[3,4-c]carbazole (DHN) scaffold.[8] The 7-oxo derivative **3** demonstrated both enzyme and cellular activity with good selectivity. However, early preclinical studies showed that it suffered from metabolic instability and poor pharmacokinetic properties. We therefore focused our attention on optimizing the potency and properties of the 5-oxo regiomer **4**. In this article, we report the optimization of positions R^2 and R^{12}, the MLK1 crystallography, the pharmacokinetic properties, and the oral in vivo activity for the MLK1 and MLK3 family-selective DHN analogs.

Chemistry

The 5-oxo carbazole analogs were synthesized via a Diels−Alder reaction as outlined in Scheme 1 using our

* To whom correspondence should be addressed. E-mail: rhudkins@cephalon.com. Tel: 610-738-6283. Fax: 610-738-6558.
† Cephalon, Incorporated.
‡ Albert Einstein College of Medicine.

10.1021/jm8005838 CCC: $40.75
Published on Web 08/21/2008

Scheme 1[a]

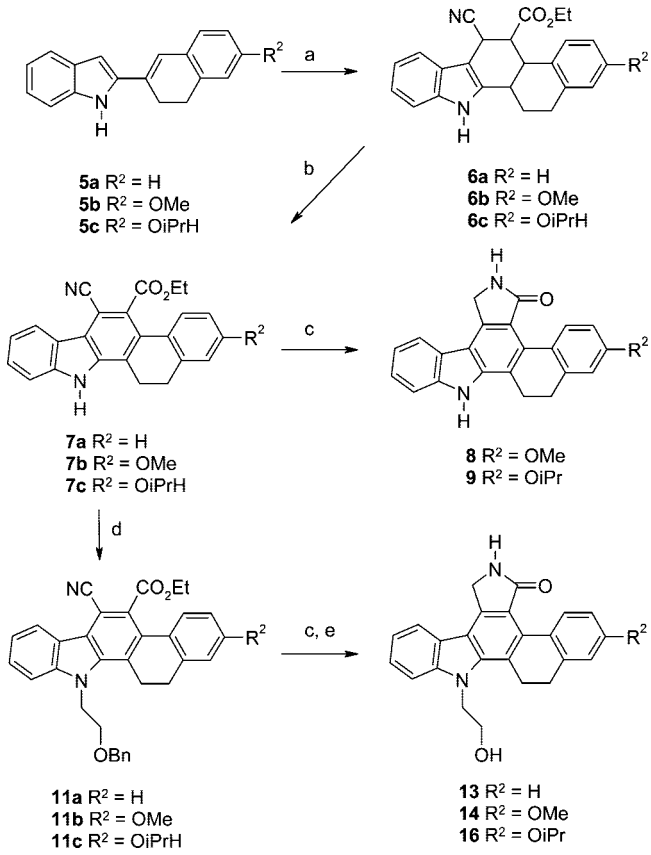

[a] Reagents and conditions: (a) ethyl *cis*-β-cyanoacrylate, $YtBr_3$, toluene; (b) DDQ, toluene, rt; (c) RaNi, H_2, DMF/MeOH → **12a**−**c**; (d) 10 N NaOH, $BrCH_2CH_2OBn$, acetone, reflux; and (e) $Pd(OH)_2$, HCl, DMF.

published methods for **3** and **4**.[8,9] The Diels−Alder reaction with ethyl *cis*-β-cyanoacrylate and 2-(3,4-dihydronaphth-2-yl)-1H-indole **5** in the presence of $YtBr_3$ in toluene proceeded in a regioselective manner to produce the 3-ethoxycarbonyl isomer **6** (Scheme 1). The aromatization of tetrahydrocarbazoles using DDQ in toluene or acetonitrile cleanly produced the cyanoester carbazoles **7**. Reductive cyclization (RaNi, H_2, DMF, MeOH) produced lactams **8** and **9**. The regiochemistry was confirmed by NMR experiments and crystallography, as previously described.[9] A key synthetic transformation in the elaboration of the N^{12} structure−activity relationships (SAR) was the clean alkylation of the indole NH by the use of NaOH in acetone without hydrolysis of the ester or nitrile. The alkylation of cyanoester carbazole **7** with 2-bromoethyl benzyl ether produced the O-benzyl-protected **11** in >90% yield. On a large scale, it was more efficient to use a two-step hydrogenation process to produce the target alcohol lactams **14** and **16** than it was to use a one-pot procedure. Accordingly, the reductive cyclization of **11a** and **11b** by the use of RaNi/H_2 in DMF/MeOH produced the O-benzyl lactam **12**. O-debenzylation using $Pd(OH)_2/H_2$ in DMF produced the alcohol lactam in high yield and purity. We needed an efficient scalable method to produce 2-hydroxy-12-ethanol **17** in high yield and purity so that it could be used as an intermediate to analog the 2-ether position. The best conditions we found to demethylate **14** were provided by a mixture of $AlCl_3$ and ethane thiol in DCE. Similar conditions were used to convert **8** to **10**. The alkylation of **17** with various alkyl halides was accomplished by the use of Cs_2CO_3 in CH_3CN or under phase-transfer conditions (NaOH, *N*-tetrabutylammonium bromide, DCM/water) to produce **18**−**22** and **24**−**26** (Scheme 2).

Results and Discussion

In Vitro MLK1 and MLK3 Structure−Activity Relationships. The MLK1 and MLK3 enzyme inhibitory data are shown in Table 1. Analogs were screened for inhibition against baculoviral glutathione-*S*-transferase (GST) fusion proteins that expressed the active human MLK1 and MLK3 kinase domains by using myelin basic protein as substrate.[6c,8] The pan-MLK inhibitor **1** was used as a reference standard, and it displayed IC_{50} values of 38 and 64 nM for MLK1 and MLK3, respectively.[5b] 5-Oxo **4** was about 30 and 11 times weaker for MLK 1 and MLK3, respectively, compared to **1** (IC_{50} = 1.1 and 0.72 μM, respectively.) A methoxy group was scanned to probe SAR around the B ring initially. This tactic revealed that the preferred position for substitution was 2 > 3 ≫ 1. Compound **8** (2-methoxy) showed a 3- to 5-fold improvement in MLK1 and MLK3 potency, whereas substitution at the 1 position was not tolerated, and the 3-OMe analog was significantly weaker (data not shown). A 2-alkoxy group proved to be important as the O*i*Pr in **9** improved potency 16-fold for MLK1 and 5-fold for MLK3 compared with **8**, whereas the 2-OH in **10** showed less than 10% inhibition at 1 μM concentration (Table 1). A set of alkanols were next installed at N^{12} in accord with our previous work that demonstrated that the chirality of the (+)K-252a 3′-sugar alcohol was critical for trkA tyrosine kinase activity.[10] Unfortunately, the ethanol analog **13** had only weak inhibitory activity versus MLK3 (IC_{50} = 1 μM, comparable in potency to **4**), whereas analogs with increased alkyl chain length or branching were devoid of activity (data not shown). Conversely, our exploring combinations of R^2-alkoxy with R^{12} ethanol produced analogs with greater-than-additive potency. Ethanol **14** and propanol **15** displayed a 10- to 15-fold improvement in MLK potency compared with **4**. The size of the O-alkyl ether at position 2 was critical for potency in the order *i*Pr > Me > *n*Pr > cAlkyl > Et > H. An optimum balance for MLK1 and MLK3 activity was obtained with R^2 OMe (**14**) (IC_{50} = 103 and 55 nM for MLK1 andMLK3, respectively) and O*i*Pr (**16**) (IC_{50} = 26 and 67 nM for MLK1 and MLK3, respectively). Substituting with larger, nonether groups at R^2 or probing the region with heterocycles or donor and acceptor groups decreased but did not abolish the activity (see **18**−**26**). (For examples, see **18**−**26**.) The R^{12} donor OH group was critical for MLK activity because O-alkyl ethers or the reomoval of the hydroxyl dramatically decreased MLK activity (data not shown).

MLK1 Cell Activity in Vitro. The potent examples **9**, **14**, **16**, and **19** were evaluated in an MLK1 cell-based assay for the inhibition of MKK4 phosphorylation. MLK1 was transfected in Chinese hamster ovary (CHO) cells with dominant-negative MKK4 cDNA, and phospho-MKK4 was measured in an ELISA-based format, as previously described.[6c,8] Compounds **14** and **16** (MLK1 enzyme IC_{50} = 26 and 103 nM, respectively) displayed MLK1 cell activity that was relatable to the isolated enzyme activity with cell IC_{50} values of 127 and 33 nM, respectively (Table 1). Compounds **9** and **19** displayed approximately 3- and 7-fold shifts from the cell free-MLK1 enzyme activity. The cell translation of **14** and **16** compared favorably to the optimized semisynthetic clinical compound **1** (MLK1 enzyme IC_{50} = 38 nM; MLK1 cell IC_{50} = 72 nM).[5b,6c]

MLK1/16 X-Ray Crystal Structure. To identify the important interactions and to assist in the design of new inhibitors,

Scheme 2[a]

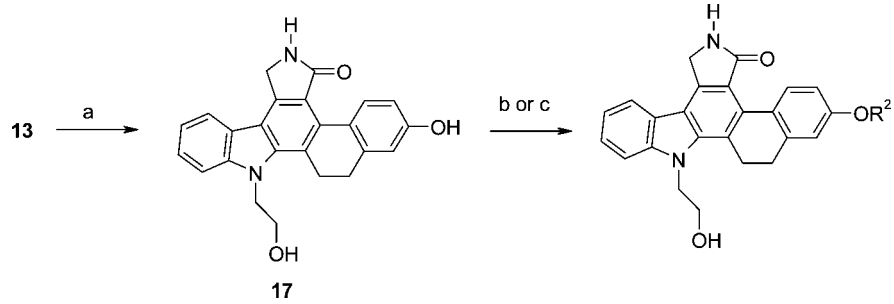

[a] Reagents and conditions: (a) (i) $AlCl_3$, EtSH, DCE, 0→50 °C, (ii) 1N HCl; (b) NaOH (1.5 equiv), *N*-tetrabutylammonium bromide, R^2−Br, CH_2Cl_2 /H_2O; and (c) R^2−Br or R^2−Cl,Ce_2CO_3, CH_3CN, 80 °C.

Table 1. MLK1 and MLK3 Activity of Dihydronaphthylcarbazole Analogs

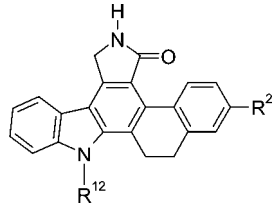

entry	R^2	R^{12}	MLK1[a]	MLK3[a]	MLK1 cells[b]
1			38	64	72
4	H	H	1106	724	
8	OMe	H	188	274	
9	O*i*Pr	H	66	159	196
10	OH	H	9%	0%	
13	H	$(CH_2)_2OH$	14%	1000	
14	OMe	$(CH_2)_2OH$	103	55	127
15	OMe	$(CH_2)_3OH$	101	87	
16	O*i*Pr	$(CH_2)_2OH$	26	65	33
17	OH	$(CH_2)_2OH$	32%	30%	
18	OCH_2cPr	$(CH_2)_2OH$	30%	32%	
19	OcPentyl	$(CH_2)_2OH$	49	32%	345
20	OcHexyl	$(CH_2)_2OH$	35%	4%	
21	OCH_2(2-Pyr)	$(CH_2)_2OH$	36%	30%	
22	$OCH_2CH_2OCH_3$	$(CH_2)_2OH$	52%	40%	
23	OCH_2CH_2OBn	$(CH_2)_2OH$	9%	0%	
24	OCH_2CH_2OH	$(CH_2)_2OH$	NT	46%	
25	OCH_2CN	$(CH_2)_2OH$	30%	8%	
26	$O(CH_2)_3CN$	$(CH_2)_2OH$	58%	46%	

[a] IC_{50} values are reported in nM as the average of duplicates agreeing within 20%; % inhibition at 1 μM. NT = not tested. [b] MLK1 cell inhibitions are IC_{50} values reported in nM, as described previously (refs 5c and 7).

Table 2. X-ray Crystallography Data Collection and Refinement Statistics[a]

Data Collection	
space group	$P2_12_12$
cell dimensions	A = 56.93, b = 126.30, c = 41.36 Å
data redundancy	5.1
unique reflns	9475
resolution (Å)[a]	2.0−2.6 (2.69−2.60)
completeness (%)[a]	96.8 (92.5)
R_{merge} (%)[a]	7.9 (31.9)
average I/σ [a]	19.3 (3.5)
Refinement	
resolution (Å)	2.0−2.6
no. reflns	
working set	8673
test set	683
R_{work}/R_{free} (%)	21.8/28.2
no. atoms	
protein	1913
solvent	43
inhibitor	32
SO_4	5
average B factor (Å^2)	33.2
rms deviations	
bond lengths (Å)	0.007
bond angles (deg)	1.42

[a] Numbers in parentheses indicate values for the highest-resolution shell.

we solved a cocrystal structure of **16** with the unphosphorylated MLK1 kinase domain (MLK1[T312A](136−406)) at 2.6 Å resolution (Table 2). This represents the first reported crystal structure that was solved in the MLK family. The topology of the MLK1 kinase domain in complex with **16** is similar to other protein kinases wherein the structure consists of a smaller N-terminal lobe, which is largely composed of β sheets, and a C-terminal lobe, which is predominantly α-helical. The N-terminal domain comprises one α helix, αC (181−197), and a six-stranded β sheet, β0 (137−139), β1 (144−150), β2 (158−163), β3 (166−174), β4 (206−211), and β5 (215−220) (Figure 2). The six-stranded β sheet is also found in GSK-3β and p38, in contrast with the five-stranded β sheet that is found in protein kinases such as FGFR, cMet, Abl, VEGFR2, CDK2, and EGFR. The additional strand β0 makes antiparallel β-sheet hydrogen bonding interactions with β5. The C-terminal lobe comprises two β strands and seven α helices. The two lobes are connected by a single-polypeptide-strand hinge region (220−224). Compound **16** is bound in the ATP pocket at the hinge in a manner that is analogous to that of **1**[11] and to the conformation of (+)K-252a (**2**) bound to the tyrosine kinase c-Met[12] (Figure 2). **16** anchors at the hinge via two key hydrogen bonds (1.8 Å); the lactam N−H forms a strong hydrogen bond with the carbonyl backbone of Gly221 and the lactam C═O accepts a hydrogen bond with the backbone amide of Ala223 (Figure 3). The MLK1 ATP pocket is formed by hydrophobic residues Ile150, Phe155, Val158, Ala169, Phe195, and Ile204 from the N-terminal lobe; Leu275 and Phe295 from the C-terminal lobe; and Met220, Phe222, and Ala223 from the hinge region. Moreover, the apolar atoms of Gly151, Gly153, Gly226, Thr293, and Asp294 also participate in the formation of the pocket. This DFG-in structure had no density in the loop between strand β and helix αC (chain segment 174−180) in the C-terminal domain and in part of the activation loop (294−319) chain segment 296−309. The binding conformation of **16** positions the 2-O-isopropyl moiety at the solvent channel where the ether oxygen forms a hydrogen bond with the Arg230 side chain (∼2.5 Å) (Figure 3). An additional hydrophobic interaction between the Phe221 side chain and the *i*Pr may account for the increased potency of **16** over **14**. The N^{12} ethanol OH serves as an H-bond donor with the carbonyl backbone of Ser272 (2.1 Å) and is also in close proximity for electrostatic contacts to the polar side-chain residue of Asn273 (∼3.4 Å) and potentially Thr293 (∼4 Å). The very flexible glycine-rich

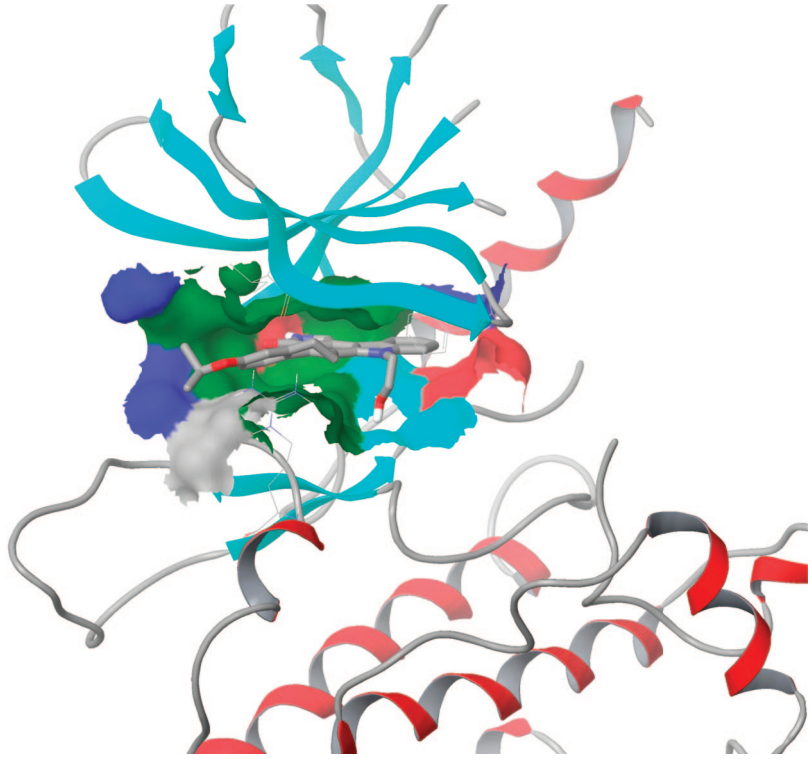

Figure 2. Ribbon diagram of the MLK1-**16** X-ray crystal structure.

Table 3. Kinase Selectivity Profile for **14** and **16**

kinase[a]	**14**	**16**	kinase[a]	**14**	**16**
MLK1	103 ± 20	26 ± 12	VEGF-R3	>10 000	2459 ± 569
MLK2	1582 ± 46	1855 ± 87	PDGF-Rβ	>10 000	>10 000
MLK3	55 ± 17	65 ± 9	FGF-R1	>10 000	>10 000
DLK	>3000	>3000	P38α	>10 000	>10 000
TrkA	1270 ± 203	1055 ± 224	IRK	>10 000	>10 000
JNK	>30 000	>30 000	EGF-R	>10 000	>10 000
MKK4/7	>3000	>3000	CDKs	>10 000	>10 000
PKC	>10 000	>6000	CHK1/2	>10 000	>10 000
VEGF-R1	>10 000	>10 000	Lck	6400	>10 000
VEGF-R2	4715 ± 603	3378 ± 585	Fyn	3400	1190

[a] IC_{50} values in nM.

nucleotide-binding loop 151−158 is closer to the active site in MLK1 compared with other kinases. A unique side-chain shift with Phe155 from the phosphorylation loop forms a hydrophobic interaction with the N12 ethyl side chain and also functions to cap the cleft and block solvent accessibility to the inhibitor.

Kinase Selectivity Profile for 14 and 16. The first-generation clinical compound **1** was a pan-MLK inhibitor with IC_{50} values of 38, 64, 23 and 114 nM for MLK1, MLK2, MLK3, and DLK, respectively.[5b,6c,8] Compound **14** had IC_{50} values of 103 and 55 nM for MLK1 and MLK3, respectively, 1.6 μM for MLK2, and >3 μM for DLK. Compound **16** had IC_{50} values of 26 and 65 nM for MLK1 and MLK3, respectively, 1.9 μM for MLK2, and >3 μM for DLK. Neither compound inhibited MLK6 or MLK7 (IC_{50} > 30 μM), which indicates a >30- to 100-fold selectivity for MLK1 or MLK3 (Table 3). Moreover, weak inhibition was demonstrated for other kinases within the stress-activated pathway, such as MKK4, MKK7, or JNK, and for serine/threonine and tyrosine kinases that are inhibited by (+)K-252a or **1**, such as protein kinase C[5c] (PKC) (mixture of Ca^{2+}-dependent isozymes α, β, and δ), vascular endothelial growth factor receptor-2 (VEGF-R2),[10b] and trkA[5c,10b,13] (Table 3). **16** markedly better demonstrated FGF-R1 (>10 μM vs 210 nM) and VEGF-R1-3 selectivity compared with clinical compound **1**, which had IC_{50} values for VEGF-1, VEGF-R2, and VEGF-R3 of 209, 43, and 39 nM, respectively. When tested against a broader panel of 254 kinases at 1 μM concentration, **14** inhibited only 4 kinases (1.6%), whereas **16** inhibited 10 kinases (3.9%) with greater than 90% inhibition.

Rat Pharmacokinetic Properties for 14 and 16. On the basis of the MLK1 and MLK3 enzyme and cellular potencies, **14** and **16** were evaluated in the rat for pharmacokinetic properties (Table 4). In a rat liver S9 preparation, both compounds showed ~44% of parents remaining after 2 h of incubation in the presence of NADPH. The oral bioavailability for **16** was estimated to be 37% by determining the AUCs following iv (1 mg/kg) and po (5 mg/kg) administration over a 6 h period. The iv terminal half life was 0.8 h with a volume of distribution of 2.0 L/kg and a clearance rate of 28 mL/min/kg. The oral C_{max} was 339 ng/mL (0.8 μM), and the brain-to-plasma ratio was approximately 0.5. Compound **14** also showed good oral bioavailability after iv (2 mg/kg) and po (4 mg/kg) administration measured over a 6 h period (F = 57%; C_{max} = 572 ng/mL) (Table 4).

In Vitro and in Vivo Activity in MPTP Models. MPTP is a potent and selective nigrostriatal DA neurotoxin that produces PD-like symptoms in humans, nonhuman primates, and mice.[14] MPP^+, the neurotoxic metabolite of MPTP, is selectively taken up in DA neurons and inhibits complex I of the mitochondrial electron transport.[15] The subsequent activation of the JNK signaling pathway leads to apoptotic neuronal death in various cell-culture models of neurodegeneration.[1,2] The MLKs function upstream of JNK to phosphorylate the dual-specificity MAPK kinases MKK4 and MKK7, which activate the MAP kinase JNK1 (see Figure 5). Correspondingly, MPP^+ addition to SH-SY5Y cells results in the activation of the JNK pathway[16] and apoptotic cell death including nuclear chromatin condensation, membrane blebbing, and DNA laddering.[17] Furthermore, MPTP administration to mice activates the JNK pathway in brain[7b] and elicits an increase in neurons with double-strand DNA breaks and chromatin clumping, which are additional markers

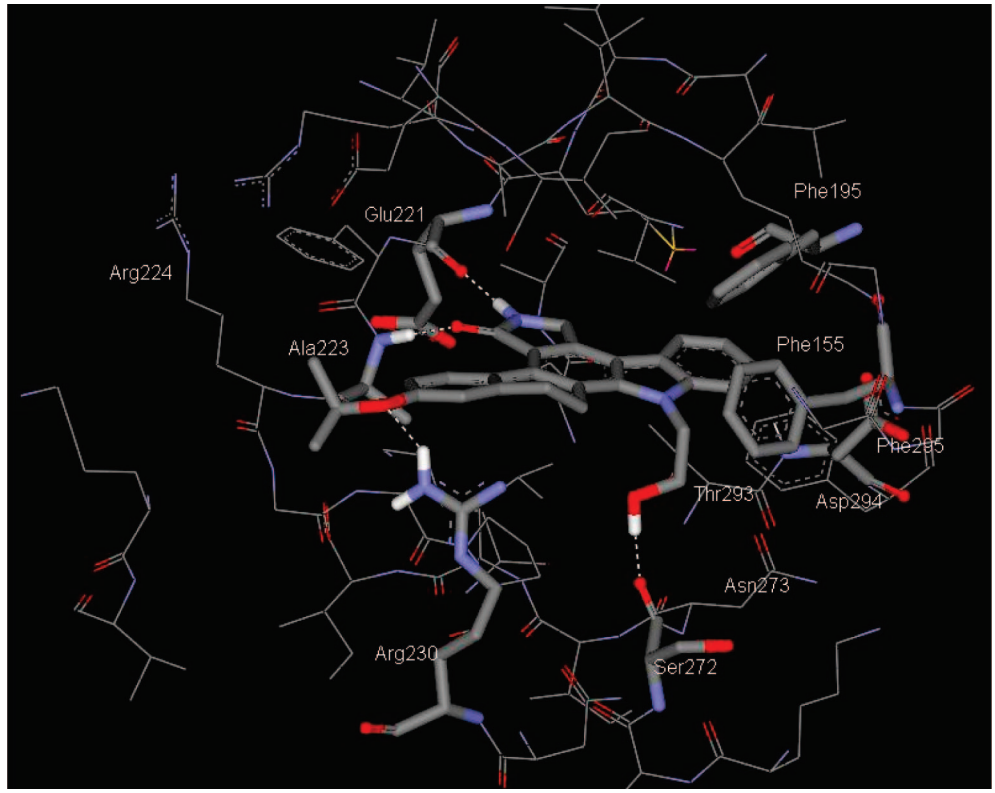

Figure 3. MLK1-**16** important interactions.

Table 4. Pharmacokinetic Properties in Rat

compd	**14**[a]	**16**[b]
iv		
$t_{1/2}$ (h)	0.6	0.8
AUC (ng·h/mL)	1731	579
Vd (L/kg)	0.9	2.0
CL (mL/min/kg)	19	28
po		
AUC (ng·h/mL)	1988	1073
C_{max} (ng/mL)	572	339
$t_{1/2}$ (h)	1.4	1.1
F (%)	57	37

[a] Administered at 2 and 4 mg/kg for iv and po, respectively. [b] Administered at 1 and 5 mg/kg for iv and po, respectivley.

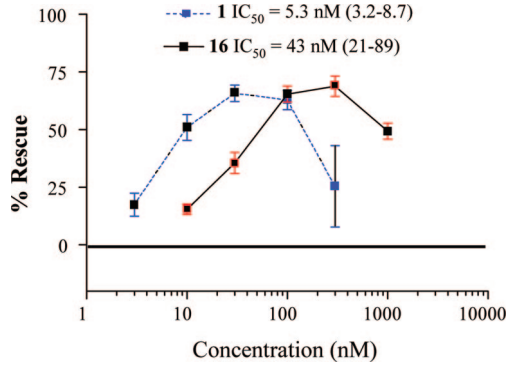

Figure 4. Activity of **1** and **16** in MPP^+-induced SH-SY5Y cell death.

of apoptosis.[18] Preclinically, **1** showed a broad neuroprotective and survival-promoting profile in vitro and in vivo.[5−7] In MPTP-induced models of PD, **1** attenuated MPP^+-mediated SH-SY5Y cell death in vitro[16a] and blocked the MPTP-mediated activation of JNK and MKK4 in a biochemical efficacy model in vivo.[7b] In neuroprotective experiments in vivo, **1** blocked the MPTP-

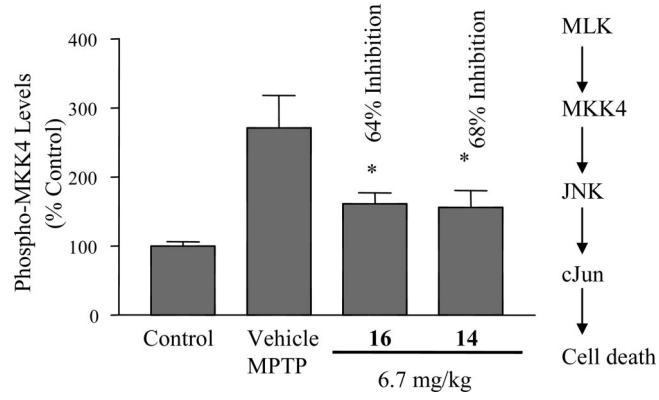

Figure 5. Activity of **14** and **16** in the MPTP-mediated increases in pMKK4 levels in mice.

induced loss of nigrostriatal dopaminergic neurons in mice[7a] and primates.[5a] **1** is a pan-MLK inhibitor and therefore cannot elucidate which MLKs are involved in the MKK4/JNK/c-Jun cell-death mechanism that is induced by MPTP. Previously, the pharmacological tools were not available to address these questions. The MLK1/3-selective inhibitors **14** and **16** were evaluated in vitro and in vivo in MPTP models of neurotoxicity. In vitro, **16** rescued human SH-SY5Y cells in a concentration-dependent manner following the treatment with MPP^+ with an IC_{50} of 43 nM.[16a] In this assay, **16** was less potent than but equally as efficacious as **1** (Figure 4). **14** displayed an IC_{50} of 32 nM. Whereas **1** showed a pronounced inverted U-shaped dose response, this effect was not seen with **14** and was only moderately seen with **16** up to 1 μM concentration, which may be a reflection of the high kinase-selectivity profile.

Previously, we reported that MPTP administration to mice increased levels of phosphoMKK4 (pMKK4) and phosphoJNK (pJNK) in the striatum and substantia nigra.[7b] Blocking the

MPTP-mediated increase in pMKK4, the immediate downstream target of the MLKs was used as a biochemical efficacy measure of peripherally administrated MLK inhibitors in the brain. Compounds **14** and **16** were administered orally at 6.7 mg/kg 2 h pre-MPTP and 2 h post-MPTP (40 mg/kg, sc). The substantia nigra from treated and control groups were dissected 2 h later, and levels of pMKK4 were measured by immunoblot.[7] **14** and **16** inhibited pMKK4 activation by 68 and 64%, respectively (Figure 5). The plasma levels 2 h postdose (4 h after MPTP) were 0.25 and 0.58 μM for **14** and **16**, respectively. For comparison, the administration of **1** at 1.0 and 10 mg/kg sc inhibited pMKK4 activation by 45−50%.[5a,7b] Similar to **1**, compounds **14** and **16** did not inhibit the MPP^+ formation via MAO-B or the extent or rate of uptake by inhibition of the DA transporter (unpublished results).

Two different models of MPTP-induced neurotoxicity can be produced by differential dosing of MPTP. The administration of a low dose (20 mg/kg sc) of MPTP produces an approximately 50% loss of striatal DA terminal markers, as measured by the specific DA uptake site ligand GBR-12935 binding, without affecting DA cell bodies in the substantia nigra, as measured by TH immunoreactivity.[5a,7a] Alternatively, the administration of a higher dose (40 mg/kg sc) results in a complete loss of striatal DA markers and about a 50% loss of substantia nigra cell bodies. Compounds **14** and **16** were evaluated for neuroprotection under both toxin-dosing conditions. The protection afforded by compound **16** was limited to striatal DA terminals after b.i.d. oral dosing in the low-dose MPTP model, whereas compound **14** protected both striatal DA terminals and cell bodies at oral doses that were as low as 2 mg/kg q.d. in the low-dose model.

Conclusions

The optimization of the R^2 and R^{12} positions of the DHN scaffold showed that combining an R^2-methoxy or an R^2-isopropoxy with an R^{12} ethanol produced analogs with greater-than-additive potency and identified **14** and **16** as potent MLK1 and MLK3 subtype-selective inhibitors. **14** and **16** demonstrated oral in vivo activity in the mouse MPTP-activated MKK4 biochemical efficacy model, which was comparable to **1**. In MPTP neuroprotection models, **14** was superior to **16** and is the subject of a pending detailed full pharmacology publication. The orally bioavailable MLK1/3 subtype inhibitors **14** and **16** are valuable tools that are helpful in delineating the critical role of the MLK kinases in the JNK pathway and in neuroprotection in various cell types and neuronal populations.

Experimental Section

Chemistry. All reagents and anhydrous solvents were obtained from commercial sources and were used as received. ^{1}H NMR specta were obtained on a Bruker 400 MHz instrument in the solvent indicated with tetramethylsilane as an internal standard. We ran preparative chromatography using silica gel GF 20 × 20 cm^2 1000 μm plates (Analtech). Coupling constants (J) are in Hertz (Hz). We ran analytical HPLC by using a Zorbax RX-C8 5 × 150 mm^2 column eluting with a mixture of acetonitrile and water containing 0.1% trifluoroacetic acid with a gradient of 10−100%.

2-(6-Methoxy-3,4-dihydronaphth-2-yl)-1H-indole (5b). To a 3 L three-necked round-bottomed flask containing indole (40.0 g, 0.4 mol) in dry THF (1.1 L) under a nitrogen atmosphere at −65 °C was added *n*-BuLi (1.6 M in hexanes, 225.3 mL). After the mixture was stirred for 1 h, CO_2(g) was passed through via a syringe for 10 min. The solution was then concentrated to half-volume at reduced pressure to remove excess CO_2. The THF (400 mL) was replaced, and *t*-BuLi (235 mL of 1.7 M solution in hexanes) was then added dropwise at −65 °C. The solution was stirred for 1 h and was treated with trimethyl borate (38.0 mL, 0.338 mol). The resulting mixture was stirred for 1 h at −65 °C. To the reaction was added Na_2CO_3 solution (338 mL of 2 M solution, 0.676 mol), dichlorobis(triphenylphosphine)-palladium(II) (1.58 g, 2.25 mmol), and 3-bromo-7-methoxy-1,2-dihydronaphthalene (55.55 g, 0.23 mol). The mixture was mechanically stirred at reflux for 18 h and was then cooled to ambient temperature (rt), and the solvent was removed at reduced pressure. The residue was dissolved in EtOAc (1.5 L) and was washed with 2 N HCl (500 mL) and water. After drying over $MgSO_4$, the EtOAc layer was evaporated to produce a tan solid. This solid was stirred in DCM/MeOH (1:1, 500 mL) for 0.5 h. The DCM was distilled at rt, and the product was collected to produce a tan solid (58.6 g, 95%). ^{1}H NMR (DMSO-d_6, δ): 11.23 (s, 1H), 7.44−7.41 (d, 1H, J = 8 Hz), 7.30−7.27 (d, 1H, J = 8 Hz), 7.05−7.00 (t, 3H, J = 7.1 Hz), 6.93−6.90 (t, 1H, J = 7 Hz), 6.73−6.69 (t, 2H, J = 7 Hz), 6.56 (s, 1H), 3.80 (s, 3H), 2.84−2.79 (t, 2H, J = 8 Hz), 2.64−2.59 (t, 2H, J = 7.7 Hz). LCMS *m*/*z*: 276 (M + 1).

2-(6-Isopropoxy-3,4-dihydronaphth-2-yl)-1H-indole (5c). This compound was prepared from indole (22.82 g, 0.16 mol) and 3-bromo-7-isopropoxy-1,2-dihydronaphthalene (34.0 g, 0.13 mol), as described for 2-(6-methoxy-3,4-dihydronaphth-2-yl)-1H-indole. The product was isolated as a tan solid (33 g, 81% yield). ^{1}H NMR (DMSO-d_6, δ): 11.22 (s, 1H), 7.44−7.41 (d, 1H, J = 8 Hz), 7.30−7.27 (d, 1H, J = 8 Hz), 7.05−7.00 (t, 3H, J = 7 Hz), 6.93−6.90 (t, 1H, J = 7 Hz), 6.73−6.69 (t, 1H, J = 7 Hz), 6.56 (s, 1H), 3.8 (m, 1H), 2.84−2.81 (t, 2H, J = 8 Hz), 2.64−2.59 (t, 2H, J = 7.8 Hz), 1.23−1.21 (d, 6H, J = 6 Hz). LCMS *m*/*z*: 304 (M + 1).

4-Cyano-3-ethoxycarbonyl-1,2,3,4-tetrahydro-(6-methoxy-1,2-dihydronaphthyl)[3,4-a]-9H-carbazole (6b). 5b (200 g, 0.726 mol), ytterbium bromide (30 g, 0.072 mol), and ethyl *cis*-β-ethyl-cyanoacrylate (272 g, 2.17 mol) in toluene (4 L) were heated at reflux for 1 h. The product that precipitated when the mixture was allowed to cool to rt was collected by filtration and was washed with toluene (400 mL) and ether (2 × 300 mL). The solid was washed thoroughly with water (3 L) and was dried to produce 165.6 g (57%) of a white solid that was used directly in the next step. LCMS *m*/*z*: 401 (M + 1).

4-Cyano-3-ethoxycarbonyl-(6-methoxy-1,2-dihydronaphthyl)[3,4-a]-9H-carbazole (7b). To **6b** (60 g, 0.150 mol) suspended in toluene (1.5 L) was added DDQ (71.4 g, 0.32 mol) at rt with vigorous stirring. The temperature of the reaction mixture gradually raised to 33 °C over 1 h before returning to rt. The solid was collected by filtration, washed thoroughly with toluene, and dried in air. It was then dispersed in 2 L of water with vigorous stirring, and 80 g of solid sodium bicarbonate was added portion-wise. After it was stirred for 3 h, the mixture was filtered, and the solid was washed thoroughly with water until the washings were a neutral pH. The solid was dried to produce 59 g (99%). mp >250 °C. ^{1}H NMR (DMSO-d_6, δ): 12.1 (s, 1H), 8.45 (d, 1H), 7.60 (m, 2H), 7.25−7.4 (m, 2H), 7.0 (s, 1H), 6.9 (s, 1H), 4.35 (q, 2H), 3.8 (s, 3H), 3.15 (m, 2H), 2.9 (m, 2H), 1.25 (t, 3H). LCMS *m*/*z*: 397 (M + 1).

2-Methoxy-13,14-dihydronaphthol[2,1-a]pyrrolo[3,4-c]carbazole-5-one (8). 7b (2.8 g, 7.1 mmol) was added to Raney nickel catalyst (ca. 2 g, wet form) in DMF/MeOH (100 mL, 3:1) and was hydrogenated at 50 psi on a Parr apparatus for 18 h. The solution was diluted with DMF (50 mL), filtered through celite, and concentrated at reduced pressure to produce 2.1 g (85%). The product was crystallized from MeOH−ether and was dried to produce a white solid. mp >250 °C. ^{1}H NMR (DMSO-d_6, δ): 11.6 (s, 1H), 8.4 (s, 1H), 7.95 (d, 1H), 7.85 (d, 1H, J = 7.8 Hz), 7.6 (d, 1H, J = 8.2 Hz), 7.45 (t, 1H, J = 7.8 Hz), 7.3 (t, 1H, J = 7.8 Hz), 6.9 (s, 1H), 6.8 (d, 1H, J = 6.6 Hz), 4.8 (s, 2H), 3.8 (s, 3H), 3.3 (t, 2H, J = 7.2 Hz), 2.87 (t, 2H, J = 5.6 Hz). LCMS *m*/*z*: 355 (M + 1). Anal. Calcd for $C_{23}H_{18}N_2O_2$ (C, H, N).

4-Cyano-3-ethoxycarbonyl-1,2,3,4-tetrahydro-(6-isopropoxy-1,2-dihydronaphthyl)-[3,4-a]-9H-carbazole (6c). This compound was synthesized using the method for **6b** by using **5c** (30 g, 0.1 mol), ytterbium bromide (4 g, 0.01 mol), and ethyl *cis*-β-ethyl

cyanoacrylate (37 g, 0.3 mol) in toluene (1 L) to produce 21.5 g (50%) of a white solid that was directly used in the next step. LCMS *m/z*: 429 (M + 1).

4-Cyano-3-ethoxycarbonyl-(6-isopropoxy-1,2-dihydronaphthyl)[3,4-a]-9H-carbazole (7c). This compound was synthesized by the method for **7b** starting with **6c** (38.4 g, 89.5 mmol) and DDQ (40.6 g, 180 mmol) in CH_3CN (1.15 L). The solid was collected, washed thoroughly with CH_3CN and water, and dried to produce 37 g (97%) of an off-white solid. mp >250 °C. ^{1}H NMR (DMSO-d_6, δ): 12.1 (s, 1H), 8.5 (d, 1H), 7.60 (m, 2H), 7.25−7.4 (m, 2H), 7.0 (s, 1H), 6.9 (s, 1H), 4.35 (q, 2H), 3.8 (m, 1H), 3.2 (m, 2H), 2.8 (m, 2H), 1.2 (m, 9H). LCMS *m/z*: 425 (M + 1).

2-Isopropoxy-13,14-dihydronaphthol[2,1-a]pyrrolo[3,4-c]carbazole-5-one (9). This compound was synthesized using the method for **8** to produce an off-white solid. mp >250 °C. ^{1}H NMR (DMSO-d_6, δ): 11.6 (s, 1H), 8.4 (s, 1H), 7.95 (d, 1H), 7.85 (d, 1H, J = 7.8 Hz), 7.6 (d, 1H, J = 8.2 Hz), 7.45 (t, 1H, J = 7.8 Hz), 7.3 (t, 1H, J = 7.8 Hz), 6.9 (s, 1H), 6.8 (d, 1H, J = 6.6 Hz), 4.8 (s, 2H), 3.7 (m, 1H), 3.3 (t, 2H, J = 7.2 Hz), 2.87 (t, 2H, J = 5.6 Hz), 1.2 (d, 6H, J = 7.2 Hz). LCMS *m/z*: 382 (M + 1). Anal. Calcd for $C_{25}H_{22}N_2O_2$ (C, H, N).

4-Cyano-3-ethoxycarbonyl-(6-methoxy-1,2-dihydronaphthyl)[3,4-a]-9−2-benzyloxyethyl-carbazole (11b). A mixture of **7b** (50 g, 0.126 mol), 2-bromoethylbenzyl ether (120 g, 0.56 mol), and 10 N NaOH (250 mL) in acetone (1450 mL) was heated at reflux for 14 h. The acetone was removed at reduced pressure, a water/hexane (500 and 1250 mL, respectively) biphase was added, and the mixture was vigorously stirred for 0.5 h. The resulting solid was collected and was thoroughly washed with water until the washing was neutral. The solid was dried under vacuum and was then washed with hexane to produce 60 g (90%) of a solid. ^{1}H NMR (DMSO-d_6, δ): 8.55 (d, 1H), 7.85 (d, 1H), 7.15 (t, 1H), 7.4 (t, 1H), 7.25 (d, 1H), 7.15 (m, 3H), 7.0 (s, 1H), 6.9 (m, 3H), 4.9 (bs, 2H), 4.30 (m, 4H), 3.8 (m, 5H), 3.45 (t, 2H), 2.75 (t, 2H), 1.2 (t, 3H). LCMS *m/z*: 531 (M + 1).

2-Methoxy-12-(2-benzyloxyethyl)-13,14-dihydronaphthol[2,1-a]pyrrolo[3,4-c]carbazole-5-one (12b). A solution of **11b** (59.8 g, 0.113 mol) in DMF/MeOH (1.1 L, 10:1) was hydrogenated over Raney nickel (100 g) at 55 psi on a Parr apparatus for 2 days. The catalyst was removed by filtration, the filtrate was concentrated under reduced pressure, and the resulting semisolid was triturated with ether (1.8 L) overnight to produce 53.6 g (93%) of a white solid that contained <3% of **14**. ^{1}HNMR (DMSO-d_6, δ): 8.45 (s, 1H), 7.95 (d, 1H), 7.85 (d, 1H), 7.7 (d, 1H), 7.50 (t, 1H), 7.3 (t, 1H), 7.15 (bq, 3H), 7.05 (bq, 2H), 6.85 (s, 1H), 6.80 (d, 1H), 4.8 (s, 2H), 3.8 (s, 3H), 3.3 (t, 2H), 2.87 (t, 2H). LCMS *m/z*: 489 (M + 1). This material was directly used in the next step without further purification.

2-Methoxy-12-(2-hydroxyethyl)-13,14-dihydronaphthol[2,1-a]pyrrolo[3,4-c]carbazole-5-one (14). A solution of **12b** (43.6 g, 89.2 mmol) in DMF (1 L) containing 5 drops of 12 M hydrochloric acid was hydrogenated over palladium hydroxide (2.2 g) at 50 psi on a Parr apparatus. The catalyst was removed by filtration through a bed of celite, and the filtrate was concentrated under reduced pressure. The resulting semisolid was triturated with ether (2 L) overnight to produce **14** as an off-white solid (36 g, 100%). mp >250 °C. ^{1}H NMR (DMSO-d_6, δ): 8.4 (s, 1H), 7.95 (d, 1H), 7.85 (d, 1H), 7.7 (d, 1H), 7.50 (t, 1H), 7.3 (t, 1H), 6.9 (s, 1H), 6.8 (d, 1H), 5.0 (bs, 1H), 4.8 (s, 2H), 4.65 (bt, 2H), 3.8 (bs, 5H), 3.3 (bt, 2H), 2.75 (bt, 2H). LCMS *m/z*: 399 (M + 1). Anal. Calcd for $C_{25}H_{22}N_2O_3$ (C, H, N).

4-Cyano-3-ethoxycarbonyl-(6-isopropoxy-1,2-dihydronaphthyl)[3,4-a]-9−2-benzyloxyethyl-carbazole (11c). This compound was synthesized using the method for **11b** starting with **7c** (35.9 g, 85 mmol), 2-bromoethylbenzyl ether (82 g, 380 mmol), and 10 N NaOH (170 mL) in acetone (1.9 L) to produce 47.2 g (97%) of an off-white solid. ^{1}H NMR (DMSO-d_6, δ): 8.5 (d, 1H), 7.85 (d, 1H), 7.55 (t, 1H), 7.4 (t, 1H), 7.3 (d, 1H), 7.2 (m, 3H), 6.95 (s, 1H), 6.9 (m, 3H), 4.9 (b, 2H), 4.75 (m, 1H), 4.30 (m, 4H), 3.8 (m, 2H), 3.3 (m, 2H), 2.75 (t, 2H), 1.2 (t, 9H). LCMS *m/z*: 559 (M + 1).

2-Isopropoxy-12-(2-benzyloxyethyl)-13,14-dihydronaphthol[2,1-a]pyrrolo[3,4-c]carbazole-5-one (12c). This compound was synthesized using the method for **12b** starting with **11c** (47.8 g, 82 mmol) to produce 41 g (97%) of a solid that contained <4% **16**. ^{1}H NMR (DMSO-d_6, δ): 8.4 (s, 1H), 7.95 (d, 1H), 7.85 (d, 1H), 7.7 (d, 1H), 7.50 (m, 1H), 7.4 (m, 1H), 7.15 (bq, 3H), 7.05 (m, 2H), 6.85 (s, 1H), 6.80 (d, 1H), 4.8 (s, m, 4H), 4.75 (m, 1H), 4.3 (s, 2H), 3.75 (m, 2H), 3.3 (m, 2H), 2.87 (t, 2H), 1.3 (d, 6H). LCMS *m/z*: 517 (M + 1). This material was directly used in the next step without further purification.

2-Isopropoxy-12-(2-hydroxyethyl)-13,14-dihydronaphthol[2,1-a]pyrrolo[3,4-c]carbazole-5-one (16). This compound was synthesized using the method for **14** starting with **12c** (41 g, 79 mmol) to produce 33 g (98%) as an off-white solid. mp >250 °C. ^{1}H NMR (DMSO-d_6, δ): 8.4 (s, 1H), 7.95 (d, 1H), 7.85 (d, 1H), 7.7 (d, 1H), 7.50 (t, 1H), 7.3 (t, 1H), 6.9 (s, 1H), 6.8 (d, 1H), 5.0 (b, 1H), 4.8 (s, 2H), 4.65 (m, 3H), 3.8 (bs, 2H), 3.3 (bt, 2H), 2.75 (bt, 2H), 1.35 (d, 6H). LCMS *m/z*: 426 (M + 1). Anal. Calcd for $C_{27}H_{26}N_2O_3$ (C, H, N).

2-Methoxy-12-(3-hydroxypropyl)-13,14-dihydronaphthol[2,1-a]pyrrolo[3,4-c]carbazole-5-one (15). This compound was synthesized using 3-bromopropylbenzyl ether and the general method for **14** to produce **15** as an off-white solid. mp >250 °C. ^{1}H NMR (DMSO-d_6, δ): 8.4 (s, 1H), 7.95 (d, 1H), 7.85 (d, 1H), 7.7 (d, 1H), 7.50 (t, 1H), 7.3 (t, 1H), 6.9 (s, 1H), 6.8 (d, 1H), 5.0 (bs, 1H), 4.8 (s, 2H), 4.65 (bt, 2H), 3.8 (m, 5H), 3.3 (m, 2H), 2.75 (m, 2H), 1.8 (m, 2H). LCMS *m/z*: 413 (M + 1).

2-Hydroxy-12-(2-hydroxyethyl)-13,14-dihydronaphthol[2,1-a]pyrrolo[3,4-c]carbazole-5-one (17). To a stirred mixture of $AlCl_3$ (800 mg, 6 mmol) in DCE (8 mL) at 0 °C was added EtSH (1.40 mL), followed by **14** (398 mg, 1 mmol). After stirring for 48 h at 50 °C, 1 N HCl (5 mL) was added and was stirred at rt for 0.5 h. The product was collected, washed with water, and dried to produce 240 mg (63%) of a tan solid. ^{1}H NMR (DMSO-d_6, δ): 9.4 (s, 1H), 8.4 (s, 1H), 7.92 (d, 1H), 7.80 (d, 1H), 7.7 (d, 1H), 7.5 (t, 1H), 7.3 (t, 1H), 6.7 (s, 1H), 6.6 (m, 1H), 5.0 (t, 1H), 4.80 (s, 2H), 4.65 (m, 2H), 3.80 (m, 2H), 3.30 (m, 2H), 2.50 (m, 2H). LCMS *m/z*: 385 (M + 1).

2-Hydroxy-13,14-dihydronaphthol[2,1-a]pyrrolo[3,4-c]carbazole-5-one (10). This compound was synthesized using the method for **17** to produce a tan solid. mp >250 °C. ^{1}H NMR (DMSO-d_6, δ): 11.6 (s, 1H), 9.45 (s, 1H), 8.3 (s, 1H), 8.06 (d, 1H, J = 5.5 Hz), 7.95 (d, 1H, J = 5 Hz), 7.55 (d, 1H, J = 5 Hz), 7.43 (t, 1H, J = 7 Hz), 7.23 (t, 1H, J = 7 Hz), 6.70 (s, 1H), 6.64 (d, 1H, J = 6 Hz), 4.8 (s, 2H), 3.3 (t, 2H, J = 7.2 Hz), 2.97 (t, 2H, J = 5 Hz). LCMS *m/z*: 340 (M − 1).

General Method for 18−20. To a mixture of **17** (38.4 mg, 0.1 mmol), NaOH (6.0 mg, 1.5 equiv), and *N*-tetrabutylammonium bromide (3.2 mg, 0.1 equiv) in 0.5 mL of CH_2Cl_2 and 0.5 mL of water was added the appropriate alkyl bromide under a N_2 atmosphere. The mixture was stirred at rt for 14−72 h and was concentrated, and the residue was washed with water and was dried over magnesium sulfate. Purification by preparative TLC with CH_2Cl_2/MeOH afforded the desired compound as solids.

2-[2-Cyclopropylmethoxy]-12-(2-hydroxyethyl)-13,14-tetrahydro-naphthol[2,1-a]pyrrolo[3,4-c]carbazole-5(6H)-one (18). ^{1}H NMR (DMSO-d_6, δ): 8.45 (s, 1H), 7.96 (d, 1H), 7.85 (d, 1H), 7.67 (d, 1H), 7.50 (t, 1H), 7.29 (t, 1H), 6.90 (s, 1H), 6.76 (d, 1H), 5.05 (m, 1H), 4.85 (s, 1H), 4.65 (m, 3H), 3.89 (m, 4H), 3.3 (m, 2H), 2.77 (m, 2H), 1.30 (m, 1H), 0.65 (m, 2H), 0.48 (m, 2H). LCMS *m/z*: 439 (M + 1).

2-[2-Cyclopentyloxy]-12-(2-hydroxyethyl)-13,14-tetrahydro-naphthol[2,1-a]pyrrolo[3,4-c]carbazole-5(6H)-one (19). ^{1}H NMR (DMSO-d_6, δ): 8.41 (s, 1H), 7.96 (d, 1H), 7.85 (d, 1H), 7.67 (d, 1H), 7.50 (t, 1H), 7.29 (t, 1H), 6.86 (s, 1H), 6.75 (d, 1H), 5.03 (m, 1H), 4.90 (m, 1H), 4.79 (s, 2H), 4.64 (m, 2H), 3.84 (m, 3H), 2.77 (m, 2H), 1.61−2.0 (m, 8H). LCMS *m/z*: 453 (M + 1).

2-Cyclohexyloxy-12-(2-hydroxyethyl)-13,14-dihydro-naphthol[2,1-a]pyrrolo[3,4-c]carbazole-5-one (20). ^{1}H NMR (DMSO-d_6, δ): 8.41(s, 1H), 7.96 (d, 1H), 7.85 (d, 1H), 7.67 (d, 1H), 7.50 (t, 1H), 7.29 (t, 1H), 6.86 (s, 1H), 6.75 (d, 1H), 5.03 (m, 1H), 4.90

(m, 1H), 4.79 (s, 2H), 4.64 (m, 2H), 3.84 (m, 4H), 2.77 (m, 2H), 1.61−2.0 (m, 10H). MS *m/z*: 467 (M + 1).

2-(2-Pyridylmethyl)-12-(2-hydroxyethyl)-13,14-dihydro-naphthol[2,1-a]pyrrolo[3,4-c]carbazole-5-one (21). A mixture of **17** (30 mg, 0.08 mmol), 2-picolyl chloride hydrochloride (20 mg, 0.12 mmol), and cesium carbonate (150 mg, 0.468 mmol) in acetonitrile (8 mL) was heated to 80 °C in a sealed tube for 18 h. The solvent was evaporated, and water was added to produce a solid, which was collected. We purified the product by silica gel preparative chromatography using ethyl acetate to produce 7 mg (19%) of a tan solid; ^{1}H NMR (DMSO-d_6, δ): 8.56 (s, 1H), 8.36 (s, 1H), 7.92 (d, 1H), 7.85 (m, 2H), 7.66 (d, 1H), 7.51 (d, 1H), 7.48 (t, 1H), 7.33 (m, 1H), 7.27 (m, 1H), 6.97 (s, 1H), 6.85 (d, 1H), 5.20 (s, 2H), 4.97 (m, 1H), 4.75 (s, 2H), 4.62 (m, 2H), 3.6−3.8 (M, 4H), 2.8 (m, 2H). LCMS *m/z*: 476 (M + 1).

2-Methoxyethoxy-12-(2-hydroxyethyl)-13,14-dihydronaphthol[2,1-a]pyrrolo[3,4-c]carbazole-5(6H)-one (22). This compound was synthesized using the method for **21** starting with **17** (50 mg, 0.013 mmol) and 2-bromoethyl methyl ether (32 mg, 0.221 mmol) to produce a tan solid (25 mg, 43%). ^{1}H NMR (DMSO-d_6, δ): 8.36 (s, 1H), 7.90 (d, 1 h), 7.83 (d, 1H), 7.64 (d, 1H), 7.45 (t, 1H), 7.24 (t, 1H), 6.87 (s, 1H), 6.77 (d, 1H), 4.97 (t, 1H), 4.75 (s, 2H), 4.61 (s, 2H), 4.11 (s, 2H), 3.77 (d, 2H), 3.65 (s, 2H), 2.73 (s, 2H). LCMS *m/z*: 443 (M + H).

2-(2-Benzyloxyethoxy)-12-(2-hydroxyethyl)-13,14-dihydronaphthol[2,1-a]pyrrolo[3,4-c]carbazole-5(6H)-one (23). This compound was synthesized using a method similar to that for **21** starting with **17** (19.5 mg, 0.05 mmol), K_2CO_3 (34.6 mg, 0.25 mmol), KI (8.7 mg, 0.52 mmol), and benzyl 2-bromoethyl ether (8.3 μL, 0.52 mmol) in acetone/DMF (2 mL; 4:1). Purification by preparative TLC using CH_2Cl_2/MeOH (95:5) afforded the product as a solid (10 mg, 39%). ^{1}H NMR (DMSO-d_6, δ): 8.5 (s, 1H), 8.0 (m, 1H), 7.90 (m, 1H), 7.7 (m, 1H), 7.5 (m, 1H), 7.3 (m, 6H), 7.0 (s, 1H), 6.9 (m, 1H), 5.0 (m, 1H), 4.80 (s, 2H), 4.65 (m, 6H), 4.05 (s, 2H), 3.80 (m, 2H), 3.30 (m, 2H), 2.50 (m, 2H). LCMS *m/z*: 519 (M + 1).

2-(2-Hydroxyethoxy)-12-(2-hydroxyethyl)-13,14-dihydronaphthol[2,1-a]pyrrolo[3,4-c]carbazole-5(6H)-one (24). A mixture of compound **23** (5 mg, 0.01 mmol), 10% $Pd(OH)_2$/C, and 0.1 mL of 12 N HCl in ethanol (1.0 mL) was hydrogenated at 42 psi on a Parr apparatus for 24 h at rt. After filtration and concentration, 2.2 mg (27%) of the product was isolated as a solid. ^{1}H NMR (DMSO-d_6, δ): 8.5 (s, 1H), 8.0 (m, 1H), 7.9 (m, 1H), 7.7 (m, 1H), 7.5 (m, 1H), 7.30 (m, 1H), 6.99 (s, 1H), 6.9 (m, 1H), 5.01 (s, 1H), 4.90 (m, 2H), 4.80 (m, 2H), 4.62 (m, 2H), 4.0 (s, 2H), 3.9 (m, 4H), 3.3 (m, 2H), 2.80 (m, 2H). LCMS *m/z*: 451(M + 1).

2-Acetonitrile-12-(2-hydroxyethyl)-13,14-dihydro-naphthol[2,1-a]pyrrolo[3,4-c]carbazole-5-one (25). This compound was synthesized using the method for **21** starting with **17** and 2-bromoacetonitrile to produce an off-white solid. ^{1}H NMR (DMSO-d_6, δ): 8.42 (s, 1H), 7.94 (m, 2H), 7.65 (m, 1H), 7.64 (m, 1H), 7.45 (t, 1H, J = 7.4 Hz), 7.26 (t, 1H, J = 7.4 Hz), 7.0 (s, 1H), 6.90 (d, 1H, J = 6.6 Hz), 5.2 (s, 2H), 4.97 (m, 1H), 4.77 (s, 2H), 4.61 (m, 2H), 3.80 (m, 2H), 3.3 (m, 2H), 2.77 (m, 2H). LCMS *m/z*: 424 (M + H).

2-(3-Butyronitrile)-12-(2-hydroxyethyl)-13,14-dihydro-naphthol[2,1-a]pyrrolo[3,4-c]carbazole-5-one (26). This compound was synthesized using the method for **21** starting with **17** and 4-bromo butyronitrile to produce an off-white solid. ^{1}H NMR (DMSO-d_6, δ): 8.36 (s, 1H), 7.82−7.92 (m, 2H), 7.64 (d, 1H, J = 8.4), 7.46 (t, 1H, J = 7.4 Hz), 7.24 (t, 1H, J = 7.5 Hz), 6.89 (s, 1H), 6.79 (d, 1H, J = 6.6 Hz), 4.97 (m, 1H), 4.75 (s, 2H), 4.61 (m, 2H), 4.07 (m, 2H), 3.80 (m, 2H), 3.3 (m, 2H), 2.62−2.73 (m, 4H), 2.0 (m, 2H). LCMS *m/z*: 452 (M + H).

Mixed-Lineage Kinase Assays. The MLK1, MLK2 and MLK assays were performed by using the Millipore multiscreen trichloroacetic acid (TCA) in-plate format, as described previously.[6c,8] Each 50 μL assay mixture contained 20 mM Hepes (pH 7.2), 5 mM EGTA, 15 mM $MgCl_2$, 1 mM DTT, 25 mM β-glycerophosphate, K_m level of ATP (60 μM for MLK1 or 100 μM for MLK2 and MLK3), 0.25 μCi [γ-^{32}P]ATP, 0.1% BSA, 2% DMSO, and 500 μg/mL myelin basic protein. The reaction was initiated by adding purified recombinant kinases (50, 150, and 100 ng of GST-$MLK1_{KD}$, GST-$MLK2_{KD/LZ}$, and GST-$MLK3_{KD}$, respectively). Samples were incubated for 15 min at 37 °C. The reaction was stopped by adding ice-cold 50% TCA, and the proteins were allowed to precipitate for 30 min at 4 °C. The plates were then washed with ice-cold 25% TCA. A supermix scintillation cocktail was added, and the plates were allowed to equilibrate for 1 to 2 h prior to counting by the Wallac 1450 MicroBeta-Plus scintillation counter. The inhibition curves were generated for the compounds by plotting percent control activity versus $\log_{10}$ of the concentration of compound. The IC_{50} values were calculated by nonlinear regression using the sigmoidal dose−response (variable slope) equation in GraphPad Prism as follows: y = bottom + (top − bottom)/(1 + 10(log IC_{50} − x) × hillslope), where y is the percent kinase activity at a given concentration of the compound, x is the logarithm of the concentration of the compound, "bottom" is the percent of control kinase activity at the highest compound concentration tested, and "top" is the percent of control kinase activity at the lowest compound concentration examined. The values for bottom and top were fixed at 0 and 100, respectively. IC_{50} values were reported as the average of duplicates that agree within 20%.

Other Kinase Assays. Inhibition assays for recombinant receptor tyrosine kinases (EGFR, FGFR1, βIRK, PDGFRβ, TIE2, TrkA, VEGF-R2) and serine/threonine kinases (CDK1, CDK2, DLK, JNK1, p38α, PKC) were performed as described previously.[10b,19,20]

Protein-Complex Preparation, Crystallization, and X-ray Data Collection. MLK1[11] (1.0 mg/mL in 20 mM HEPES, 25 mM NaCl, 1 mM DTT, and 1 mM EDTA (pH 7.4)) was incubated with 1 mM **16** for 30 min at 4 °C. Cocrystals of the enzyme[11] and **16** were obtained by mixing 2 μL of the protein complex (1.7 mg/ml) in 20 mM HEPES (pH 7.4), 25 mM NaCl, 1 mM DTT, and 1mM EDTA with 1 μL of the reservoir solution of 12% PEG20000, 200 mM $Am_2(SO_4)$, and 100 mM MES (pH 6.5). The prepared complex was crystallized by hanging-drop vapor diffusion by combining 3 μL of the protein−ligand solution with 1 μL of a reservoir solution containing 20% PEG 3350 and 0.2 M $MgSO_4$ (pH 5.9). The crystals appeared in 5 to 6 days as thin plates and exhibited diffraction that was consistent with that of the orthorhombic space group $P2_12_12$ (a = 56.93, b = 126.30, and c = 41.36 Å) with 1 molecule of enzyme−inhibitor complex per asymmetric unit. Prior to data collection, the crystals were transferred to cryoprotectant solutions composed of their mother liquors and 20% glycerol. After incubation for about 15 s, the crystals were flash-cooled in a nitrogen stream. X-ray diffraction data were collected at 2.6 Å resolution at the NSLS X4A beamline (Brookhaven National Laboratory) on an ADSC CCD detector. We integrated and scaled diffraction intensities by using the Denzo and Scalepack programs.[21] The final 2.6 Å data set for the crystal of the complex was 96.8% complete with an R_{merge} of 0.079 (Table 2).

Structure Determination and Model Refinement. The structure of the MLK1-**16** complex was solved by molecular replacement using the EPMR program.[22] The APO-MLK1 monomer structure (unpublished results) was used as the search model. The solution was found as one clear monomer in a search that used all data between 15 and 4 Å. The model was subsequently refined with CNS.[23] Bound **16** could be clearly seen in the electron-density maps immediately after the first cycle of rigid-body refinement of the protein molecule alone. Iterative cycles of manual rebuilding with TOM[24] and refinement with CNS resulted in a model of the complex at R_{cryst} = 0.218 and R_{free}= 0.282. The final structure contains 1913 protein atoms, one inhibitor molecule, one SO_4^{-2} ion and 43 water molecules for a single monomer of the complex in the asymmetric unit. None of the nonglycine residues lie in the disallowed regions of the Ramachandran plot. The X-ray data collection and crystallographic refinement statistics are represented in Table 2.

Coordinates. The coordinates for MLK1-**16** have been deposited in the Protein Data Bank (PDB code is 3DTC).

Rat Pharmacokinetics. Adult male Sprague−Dawley (Charles River, Kingston, NY) rats (n = 3/treatment group) were dosed via

the lateral tail vein with the indicated dose for intravenous administration (3% DMSO, 30% solutol, and 67% phosphate-buffered saline) or via oral gavage (50% Tween 80, 40% propylene carbonate, and 10% propylene glycol) at the indicated dose. Rats were fasted overnight prior to oral dose administration. Serial blood samples were collected from the lateral tail vein in heparinized collection tubes (approximately 0.25 mL) at seven sampling times over a 6 h period. The plasma was separated by centrifugation, and the sample was prepared for analysis HPLC/MS by protein precipitation with acetonitrile. The plasma samples were analyzed for drug and internal standard via LCMS/MS protocol. The pharmacokinetic parameters were calculated by a noncompartmental method using WinNonlin software (professional version 4.1, Pharsight Corporation, Palo Alto, CA, 1997).

Acknowledgment. We acknowledge technical support from George Gessner, Thomas Connors, Shi Yang, Beth McKenna, and Beth Ann Thomas and insightful discussions and support from Drs. Jeffry Vaught and Ed Bacon from Cephalon, Inc. and Ejner Moltzen and Erik Nielsen from Lundbeck A/S.

Supporting Information Available: Elemental analysis of key compounds. This material is available free of charge via the Internet at http://pubs.acs.org.

References

(1) (a) Maroney, A. C.; Saporito, M. A.; Hudkins, R. L. Mixed lineage kinase family, potential targets for preventing neurodegeneration. *Curr. Med. Chem.: Cent. Nerv. Syst. Agents* **2002**, *2*, 143–155. (b) Wang, L. H.; Besirli, C. G.; Johnson, E., Jr. Mixed lineage kinases: a target for the prevention of neurodegeneration. *Annu. Rev. Pharmacol. Toxicol.* **2004**, *44*, 451–474. (c) Gallo, K. A.; Johnson, G. L. Mixed-lineage kinase control of JNK and p38 MAPK pathways. *Nat. Rev. Mol. Cell. Biol.* **2002**, *3*, 663–672.

(2) (a) Bozyczko-Coyne, D.; Saporito, M. S.; Hudkins, R. L. Targeting the JNK pathway for therapeutic benefit in CNS disease. *Curr. Drug Targets: CNS Neurol.Disord.* **2002**, *1*, 31–49. (b) Bogoyevitch, M. A.; Boehm, I.; Oakley, A.; Ketterman, A. J.; Barr, R. K. Targeting the JNK MAPK cascade for inhibition: basic science and therapeutic potential. *Biochim. Biophys. Acta* **2004**, *1697*, 89–101. (c) Harper, S. J.; LoGrasso, P. Signaling for survival and death in neurons. The role of stress-activated kinases, JNK and p38. *Cell. Signalling* **2001**, *13*, 299–310. (d) Mielke, K.; Herdegen, T. JNK and p28 stress kinases: degenerative effectors of signal-transduction-cascades in the nervous system. *Prog. Neurobiol.* **2000**, *61*, 45–60.

(3) (a) Gupta, S.; Barrett, T.; Whitmarsh, A. J.; Cavanagh, J.; Sluss, H. K.; Derijard, B.; Davis, R. J. Selective interaction of JNK protein kinase isoforms with transcription factors. *EMBO J.* **1996**, *15*, 2760–2770. (b) Kallunki, T.; Su, B.; Tsigelny, I.; Sluss, H. K.; Derijard, B.; Moore, G.; Davis, R.; Karin, M. JNK2 contains a specificity-determining region responsible for efficient c-Jun binding and phosphorylation. *Genes Dev.* **1994**, *8*, 2996–3007. (c) Kallunki, T.; Deng, T.; Hibi, M.; Karin, M. c-Jun can recruit JNK to phosphorylate dimerization partners via specific docking interactions. *Cell* **1996**, *87*, 1–20.

(4) (a) Hirsch, E. C.; Hunot, S.; Faucheux, B.; Agid, Y.; Mizuno, Y.; Mochizuki, H.; Tatton, W. G.; Tatton, N.; Olanow, W. C. Dopaminergic neurons degenerate by apoptosis in Parkinson's disease. *Mov. Disord.* **1999**, *14*, 383–385. (b) Hartman, A.; Hunot, S.; Michel, P. P.; Muriel, M. P.; Vyas, S.; Faucheux, B.; Mouatt-Prigent, A.; Turmel, H.; Srinivasan, A.; Ruberg, M.; Evan, G. I.; Agid, Y.; Hirsch, E. C. Caspace-3: a vulnerability factor and final effector in apoptotic death of dopaminergic neurons in Parkinson's disease. *Proc. Natl. Acad. Sci. U.S.A.* **2000**, *97*, 2875–2880.

(5) (a) Saporito, M. A.; Hudkins, R. L.; Maroney, A. C. Discovery of CEP-1347/KT-7515: an inhibitor of the cJun N-terminal kinase pathway for the treatment of neurodegenerative diseases. *Prog. Med. Chem.* **2002**, *40*, 23–62. (b) Murakata, C.; Kaneko, M.; Gessner, G.; Angeles, T. S.; Ator, M. A.; O'Kane, T. M.; McKenna, B. A. W.; Thomas, B. A.; Mathiasen, J. R.; Saporito, M. S.; Bozyczko-Coyne, D.; Hudkins, R. L. Mixed lineage kinase activity of indolocarbazole analogs. *Bioorg. Med. Chem. Lett.* **2002**, *12*, 147–150. (c) Kaneko, M.; Saito, Y.; Saito, H.; Matsumoto, T.; Matsuda, Y.; Vaught, J. L.; Dionne, C. A.; Angeles, T. S.; Glicksman, M. A.; Neff, N. T.; Rotella, D. P.; Kauer, J. C.; Mallamo, J. P.; Hudkins, R. L.; Murakata, C. Neurotrophic 3,9-bis[(alkylthiomethyl]- and -[bis(alkoxymethyl)]-K-252a Derivatives. *J. Med. Chem.* **1997**, *40*, 1863–1869.

(6) (a) Glicksman, M. A.; Chiu, A. Y.; Dionne, C. A.; Kaneko, M.; Murakata, C.; Oppenheim, R. W.; Prevette, D.; Sengelaub, D. R.; Vaught, J. L.; Neff, N. T. CEP-1347/KT7515 prevents motor neuronal programmed cell death and injury-induced dedifferentiation in vivo. *J. Neurobiol.* **1998**, *35*, 361–370. (b) Borasio, G. D.; Hostmann, S.; Anneser, J. M. H.; Neff, N. T.; Glicksman, M. A. CEP-1347/KT7515, a JNK pathway inhibitor, supports the in vitro survival of chick embryonic neurons. *NeuroReport* **1998**, *9*, 1435–1439. (c) Maroney, A. C.; Finn, J. P.; Connors, T. J.; Durkin, J. T.; Angeles, T.; Gessner, G.; Xu, Z.; Meyer, S. L.; Savage, M. J.; Greene, L. A.; Scott, R. W.; Vaught, J. L. CEP-1347 (KT-7515), a semisynthetic inhibitor of the mixed lineage kinase family. *J. Biol. Chem.* **2001**, *276*, 25302–25308.

(7) (a) Saporito, M. S.; Brown, E. M.; Miller, M. S.; Carswell, S. CEP-1347/KT7515, an inhibitor of c-Jun N-terminal kinase activation, attenuates the 1-methyl-4-phenyl tetrahydropyridine-mediated loss of nigrostriatal dopaminergic neurons in vivo. *J. Pharmacol. Exp. Ther.* **1999**, *288*, 421–427. (b) Saporito, M. S.; Thomas, B. A.; Scott, R. W. MPTP activates c-jun NH_2-terminal kinase (JNK) and its upstream regulator kinse MKK4 in nigrostriatal neurons in vivo. *J. Neurochem.* **2000**, *75*, 1200–1208.

(8) Hudkins, R. L.; Johnson, N. W.; Angeles, T. S.; Gessner, G.; Mallamo, J. P. Synthesis and mixed lineage kinase activity of pyrrolocarbazole and isoindolone analogs of (+)K-252. *J. Med. Chem.* **2007**, *50*, 433–441.

(9) Hudkins, R. L.; Park, C.-H. Synthesis of indeno[2,1-a]pyrrolo[3,4-c]carbazole lactam regioisomers using ethylcis-β-cyanoacrylate as a dienophile and lactam precursor. *J. Heterocycl. Chem.* **2003**, *40*, 135–142.

(10) (a) Gingrich, D. E.; Hudkins, R. L. Synthesis and kinase inhibitory activity of 3′-(*S*)-*epi*-K-252a. *Bioorg. Med. Chem. Lett.* **2002**, *12*, 2829–2831. (b) Gingrich, D. L.; Yang, S. X.; Gessner, G. W.; Angeles, T. S.; Hudkins, R. L. Synthesis, modeling and *in vitro* activity of 3′-(*S*)-*epi*-K-252a analogs. Elucidating the stereochemical requirements of the 3′-sugar alcohol on trkA tyrosine kinase activity. *J. Med. Chem.* **2005**, *48*, 3776–3783.

(11) The CEP-1347-MLK1 and apo-MLK1 crystal structures are the subject of a separate publication.

(12) Schiering, N.; Knapp, S.; Marconi, M.; Flocco, M. M.; Cui, J.; Perego, R.; Rusconi, L.; Cristiani, C. Crystal structure of the tyrosine kinase domain of the hepatocyte growth factor receptor c-Met and its complex with the microbial alkaloid K-252a. *Proc. Natl. Acad. Sci. U.S.A.* **2003**, *22*, 12654–12659.

(13) Ruggeri, B. A.; Miknyoczki, S. J.; Singh, J.; Hudkins, R. L. The role of neurotrophin-trk interactions in oncology: The antitumor efficacy of potent and selective trk tyrosine kinase inhibitors on preclinical tumor models. *Curr. Med. Chem.* **1999**, *6*, 845–857.

(14) (a) Langston, J. W. The etiology of Parkinson's disease with emphasis on the MPTP story. *Neurology* **1996**, *47*, S153−S160. (b) Heikkila, R. E.; Manzino, L.; Cabbat, F. S.; Duvoisin, R. C. Protection against the dopaminergic neurotoxicity of 1-methyl-4-phenyl-1,2,3,6-tetrahydropyridine by monoamine oxidase inhibitors. *Nature* **1984**, *311*, 467–469. (c) Heikkila, R. E.; Hess, A.; Duvoisin, R. C. Dopaminergic neurotoxicity of 1-methyl-4-phenyl-1,2,3,6-tetrahydropyridine in mice. *Science* **1984**, *224*, 1451–1453. (d) Blanchet, P. J.; Konitsiotis, S.; Hyland, K.; Arnold, L. A.; Pettigrew, K. D.; Chase, T. N. Chronic exposure to MPTP as a primate model of progressive Parkinsonism: a pilot study with a free radical scavenger. *Exp. Neurol.* **1998**, *153*, 214–222.

(15) Nicklas, W. J.; Vyas, I.; Heikkila, R. E. Inhibition of NADH-linked oxidation in brain mitochondria by 1-methyl-4-phenylpyridine, a metabolite of the neurotoxin, 1-methyl-4-phenylpyridine. *Life Sci.* **1985**, *36*, 2503–2508.

(16) (a) Mathiasen, J. R.; McKenna, B. A. W.; Saporito, M. S.; Ghadge, G. D.; Roos, R. P.; Holskin, B. P.; Wu, Z.-L.; Trusko, S. P.; Connors, T. P.; Maroney, A. C.; Thomas, B. A.; Thomas, J. C.; Bozyczko-Coyne, D. Inhibition of mixed lineage kinase 3 attenuates MPP^+-induced neurotoxicity in SH-SY5Y cells. *Brain Res.* **2004**, *1003*, 86–97. (b) Cassarino, D. S.; Halvorsen, E. M.; Swerdlow, R. H.; Abramova, N. N.; Parker, W. D., Jr.; Sturgill, T. W.; Bennett, J. P., Jr. Interaction among mitochondria, mitogen-activated protein kinases and nuclear factor kB in cellular models of Parkinson's disease. *J. Neurochem.* **2000**, *74*, 1384–1392.

(17) (a) Sheehan, J. P.; Palmer, P. E.; Helm, G. A.; Tuttle, J. B. MPP^+ induced apoptotic cell death in SH-SY5Y neuroblastoma cells: an electron microscope study. *J. Neurosci. Res.* **1997**, *48*, 226–37. (b) Dipasquale, B.; Marini, A. M.; Youle, R. J. Apoptosis and DNA degradation induced by 1-methyl-4-phenylpyridinium in neurons. *Biochem. Biophys. Res. Commun.* **1991**, *181*, 1442–1448.

(18) Tatton, N. A.; Kish, S. J. In situ detection of apoptotic nuclei in the substantia nigra compacta of 1-methyl-4-phenyl-1,2,3,6-tetrahydropyridine-treated mice using terminal deoxynucleotidyl transferase labelling and acridine orange staining. *Neuroscience* **1997**, *77*, 1037–1048.

(19) Angeles, T. S.; Steffler, C.; Bartlett, B. A.; Hudkins, R. L.; Stephens, R. M.; Kaplan, D. R.; Dionne, C. A. Enzyme linked immunosorbant

assay for TrkA tyrosine kinase activity. *Anal. Biochem.* **1996**, *236*, 49–55.

(20) Ruggeri, B.; Singh, J.; Gingrich, D.; Angeles, T.; Albom, M.; Chang, H.; Robinson, C.; Hunter, K.; Dobrzanski, P.; Jones-Bolin, S.; Aimone, L.; Klein-Szanto, A.; Herbert, J.-M.; Bono, F.; Casellas, P.; Bourie, B.; Pili, R.; Isaacs, J.; Ator, M.; Hudkins, R.; Dionne, C.; Mallamo, J.; Vaught, J. CEP-7055: a novel, orally-active pan inhibitor of vascular endothelial growth factor receptor tyrosine kinases with potent anti-angiogenic activity and anti-tumor efficacy in pre-clinical models. *Cancer Res.* **2003**, *63*, 5978–5991.

(21) Otwinowski, Z.; Minor, W. Processing of X-ray Diffraction Data Collected in Oscillation Mode. In *Methods in Enzymology*; Carter, C. W. J., Sweet, R. M., Abelson, J. N., Simon, M. I., Eds.; Academic Press: New York, 1997; 307−326.

(22) Kissinger, C. R.; Gehlhaar, D. K.; Fogel, D. B. Rapid automated molecular replacement by evolutionary search. *Acta Crystallogr., Sect. D: Biol. Crystallogr.* **1999**, *55*, 484–491.

(23) Jones, A. T. Interactive computer graphics: FRODO. *Methods Enzymol.* **1985**, *115*, 157–171.

(24) Brunger, A. T.; Adams, P. D.; Clore, G. M.; DeLano, W. L.; Gros, P.; Grosse-Kunstleve, R. W.; Jiang, J. S.; Kuszewski, J.; Nilges, M.; Pannu, N. S.; Read, R. J.; Rice, L. M.; Simonson, T.; Warren, G. L. Crystallography & NMR system: Aa new software suite for macromolecular structure determination. *Acta Crystallogr., Sect. D: Biol. Crystallogr.* **1998**, *54*, 905–921.

JM8005838